Progress In Electromagnetics Research C, Vol. 123, 227–236, 2022

Development of a Low Profile Wideband SIW Cavity-Backed I-Shaped Slot Antenna

Anil Kumar Katta[1, *] and Praveen Babu Choppala[2]

Abstract—In this paper, a bandwidth improvement technique in substrate integrated waveguide (SIW) slotted antennas is presented. Here, wideband is achieved by using a single cavity mode (TE_{210}) instead of multiple cavity modes, which is the most distinct approach as compared to other SIW based antennas. When the rectangle slot is loaded at bottom surface of the cavity, the TE_{210} cavity mode of the antenna is perturbed. As a result, two independent modes namely odd TE_{210} and even TE_{210} are successfully generated and merged in close proximity. Consequently, an impedance bandwidth of 12.8% is obtained. When a vertical slit is added at each end of the rectangle slot to make as an I-shaped slot, the impedance bandwidth is increased from 12.8% to 13.94%. The fabricated antenna shows the measured impedance bandwidth of 14.4% and exhibits a gain of 5 dBi to 7 dBi throughout the operating band. The proposed design still retains many features such as light weight, easy fabrication, and easy integration.

1. INTRODUCTION

Printed slot antennas with light weight, easy fabrication, easy integration, unidirectional radiation, and high impedance bandwidth are in high demand for microwave and millimeter-wave frequency range [1–4]. Substrate integrated technology (SIW) realizes conventional cavity-backed antennas in planar form. The outstanding features of SIW are high-density integration with conventional planar components (e.g., microstrip lines and coplanar waveguides), easy manufacturing, and low power losses [5–8]. Several planar slot antennas have been reported in the literature on the basis of SIW technology. A low-profile printed slot antenna on the basis of SIW technique is described in [9], which generates the radiation by TE_{120} mode of the cavity at 10 GHz. Due to high quality factor (Q), the bandwidth is only 1.7% with a gain of 5.3 dBi.

In [10], the bandwidth of 6.3% is obtained by combining the two-hybrid modes of the cavity in close proximity. In [11], offset feeding method is used to excite the TE_{120} mode, which results in an impedance bandwidth of 4.2%. In [12], the modified bow-tie slot excites both TE_{110} and TE_{120} modes of the SIW cavity to improve the bandwidth up to 9.4%. The demeanor of the hybrid modes in [10] is the same as that of [12]. In [13], a method of corner perturbation in the square cavity enhances the bandwidth (1.65%). In [14], the matching slot excites the TE_{210} mode to attain the bandwidth up to 8%. In [15], the TM_{010} mode of the patch improves the impedance bandwidth.

In [16], multi-resonant slots achieve a bandwidth up to 11%. In [17], bandwidth is improved by cutting the edges of the SIW cavity with a circular shape. Bandwidth enhancement is obtained by using bilateral slots [18], a butterfly-shaped slot with SIW circular cavity [19], and a bow-tie shaped slot [20]. In [21], a novel wideband hexagonal cavity-backed slot antenna is discussed, where the antenna achieves the −10 dB bandwidth of 14%. Several papers report bandwidth enhancement, by using two shorting vias [22], using stacked cavities [23], exciting the modes of the patch [24], antenna array [25],

Received 26 July 2022, Accepted 25 August 2022, Scheduled 5 September 2022

* Corresponding author: Anil Kumar Katta (anilecedepartment@gmail.com).

[1] Department of ECE, AU College of Engineering, Andhra University, Visakhapatnam, Andhra Pradesh, India. [2] Department of ECE, Wellfare Institute of Science Technology & Management, Andhra University, Visakhapatnam, Andhra Pradesh, India.

single metallic via-hole above the slot [26], removal of the substrate underneath the slot [27], balanced shorting vias below the rectangle slot [28], and unbalanced shorting vias [29].

In this paper, bandwidth is improved by perturbing a TE_{210} mode instead of multiple modes as compared to the methods reported in [10–25]. Due to the strong loading of an I-shaped slot, the TE_{210} cavity mode is perturbed. Consequently, two independent modes (odd TE_{210}, even TE_{210}) are successfully generated. Then an impedance bandwidth of 13.94% can be obtained by merging these modes in close proximity. The measured front-to-back ratio (FTBR) is about 13 dB and 19 dB, respectively, at 9.6 GHz and 10.6 GHz. It also results in high gain and unidirectional pattern.

2. ANTENNA DESIGN

Figure 1 illustrates the configuration of the proposed antenna, which mainly comprises a dielectric substrate, SIW cavity, radiating slot, and feeding circuit. The design steps of the proposed antenna are depicted in Figure 2. The entire antenna is designed and fabricated on RT/duroid 5880 dielectric material ($\varepsilon_r = 2.2$, $\tan\delta = 0.0009$). It begins with a microstrip line fed SIW cavity and followed by rectangle slot loading. Later, the SIW cavity is loaded with an I-shaped slot.

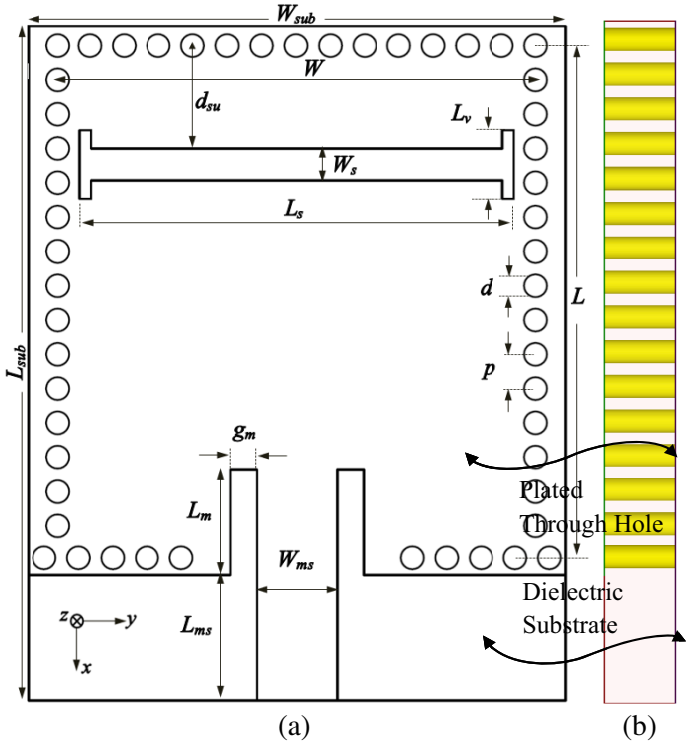

Figure 1. Proposed antenna. (a) Configuration. (b) Side view [$W_{sub} = 23.5$, $L_{sub} = 29.5$, $W = 20.9$, $L = 22.4$, $L_s = 19$, $W_s = 1.4$, $L_v = 3$, $d_{su} = 4.55$, $L_m = 4.6$, $g_m = 1.15$, $W_{ms} = 3.5$, $L_{ms} = 5.5$, $d = 1$, $p = 1.5$, $h = 1.57$] (Units: mm).

The SIW cavity portrayed in Figure 2(a) is fully created on a single PCB of height h, where cavity side walls are set up by implanting multiple plated through holes along the edges of the substrate. To emulate the conventional cavity, the pitch (p) and post diameter (d) must follow the conditions $d/p \geq 0.5$ and $d/\lambda_0 \leq 0.1$ to reduce the power losses, where λ_0 refers to the free space wavelength at 10 GHz. The Ansoft HFSS is utilized to design the proposed antenna. The dimensions of the 50 Ω microstrip feeding line and the antenna are related to the resonant frequency of the antenna. The size

of the SIW cavity is approximately designed by the resonant frequency [30]:

$$f_r(TE_{mnp'}) = \frac{1}{2\sqrt{\mu_0\varepsilon_0\varepsilon_r}}\sqrt{\left(\frac{m}{L_{eff}}\right)^2 + \left(\frac{n}{W_{eff}}\right)^2 + \left(\frac{p'}{h}\right)^2} \quad (1)$$

where m, n, and $p\prime$ are the number of half wave sinusoidal cycles, equivalent length, and width of the cavity (L_{eff} or W_{eff}) $= L$ or $W - \frac{d^2}{0.95*p}$, respectively, ε_r — relative permittivity, d — diameter of each plated hole, and p — distance between the adjacent metal through holes (pitch).

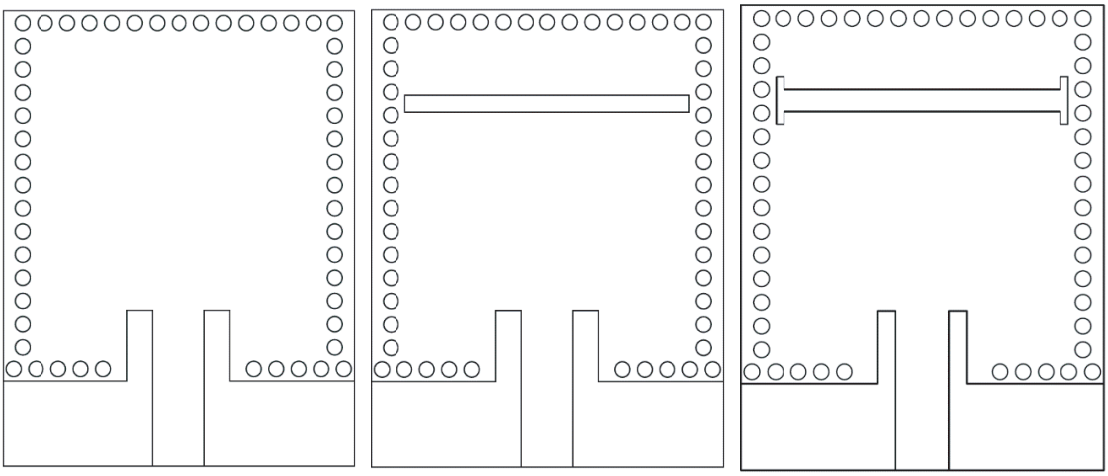

Figure 2. Design steps of the proposed antenna. (a) SIW cavity (Step I). (b) Rectangle slot (Step II). (c) I-shaped slot (Step III).

Initially, a rectangular slot with the size of $L_s \times W_s$ is considered on the ground plane as shown in Figure 2(b). It acts as a main radiating element to the antenna and is positioned by distance d_{su} from the upper lateral wall of the cavity. To further improve the bandwidth, each end of the rectangular slot is made by protruded lengths to form an I-shaped slot as shown in Figure 2(c). The rectangular slot length is determined by using the formula given in Equation (2).

$$l_s = \frac{c}{2f_1\sqrt{\varepsilon}_{eff}}; \quad \varepsilon_{eff} = (\varepsilon_r + 1)/2 \quad (2)$$

where l_s — slot length, ε_{eff} — slot equivalent permittivity, c — speed of light in the free space, f_1 — resonant frequency of the TE_{110} mode.

3. WORKING PRINCIPLE

In order to understand the working mechanism, the simulation of the SIW cavity is explicated first. Figure 3 epitomizes the input resistance curve ($\mathrm{Re}(Z_{11})$) of the proposed design, which certifies the wideband impedance matching properties and is also used for recognizing the modes of the SIW cavity. The antenna excites the SIW cavity through a microstrip line, and as a result, the dominant mode (TE_{110}) at 6.85 GHz and TE_{210} mode at 10.2 GHz are developed. For TE_{110} and TE_{210} modes of the SIW cavity, the direction of E-field is perpendicular to the top and bottom conductive surfaces while the direction of the H-field is parallel to the top and bottom conductive layers. Figures 4(a)–(b) illustrate the distribution of the electric field in the cavity for the TE_{110} and TE_{210} modes.

When the rectangular slot is loaded at the bottom surface of the cavity, the SIW cavity modes mentioned above get perturbed. As a result, the dominant TE_{110} mode moves downward to 6.1 GHz. In a similar manner, due to perturbations in TE_{210} mode, two independent modes, odd TE_{210} and even TE_{210}, are excited at 9.55 GHz and 10.85 GHz, respectively. The position of the slot is kept in

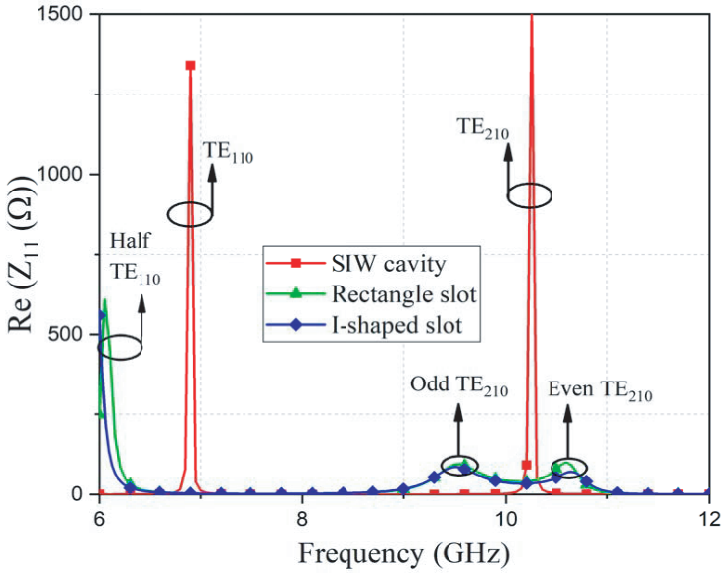

Figure 3. Input resistance (Real (Z_{11})) plot of the cavity without and with slot loading.

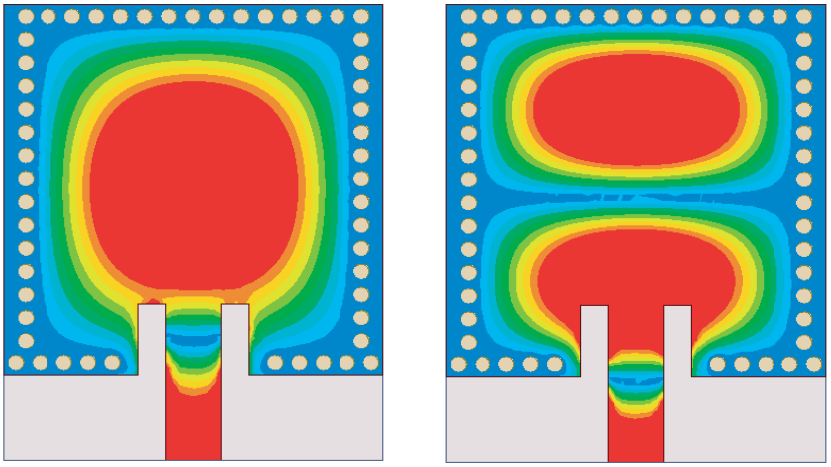

Figure 4. Distribution of E-field in the SIW cavity. (a) 6.85 GHz, TE_{110} mode. (b) 10.2 GHz, TE_{210} mode.

such a way that to merge the said independent modes close to each other, enhanced bandwidth can be obtained. Step II shows wide impedance bandwidth, ranging from 9.5 GHz to 10.8 GHz (1.3 GHz). Moreover, the additional protruded lengths exist at each end of the rectangle slot aiming to improve the impedance matching and radiation performance in the proposed design (Step III). The protruded lengths of each end of the rectangle slot decrease the overall quality factor. As a result, the bandwidth of the antenna is improved. The antenna shows double resonances at 9.6 GHz and 10.6 GHz with an impedance bandwidth, ranging from 9.34 GHz to 10.74 GHz (1.4 GHz). It can also be observed from Figure 3 that the above-mentioned modes remain almost unperturbed. Figures 5(a)–(c) depict magnitude distributions of the E-field in the SIW cavity with an I-shaped slot.

Figures 6(a)–(b) illustrate the current distributions of the proposed antenna at 9.6 GHz and 10.6 GHz. At both resonances, the current is mostly focused on the upper half of the SIW cavity above the slot with a minimum in the lower half. It is likewise seen that, at the first resonance, the maximal current flows to the upper edge of the slot while at the second resonance, the maximal current

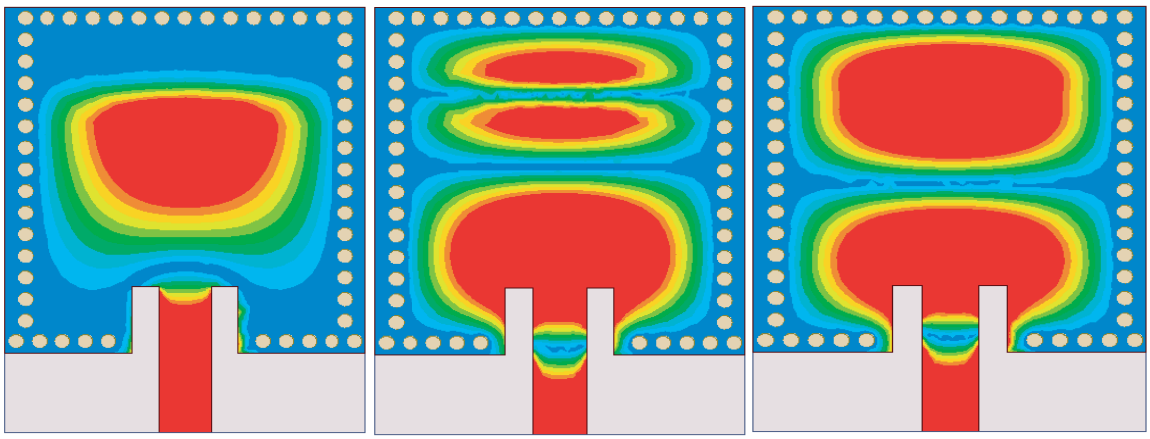

Figure 5. Distribution of E-field across the I-shaped slot. (a) 6 GHz, half TE_{110} mode. (b) 9.5 GHz, odd TE_{210} mode. (c) 10.65 GHz, even TE_{210} mode.

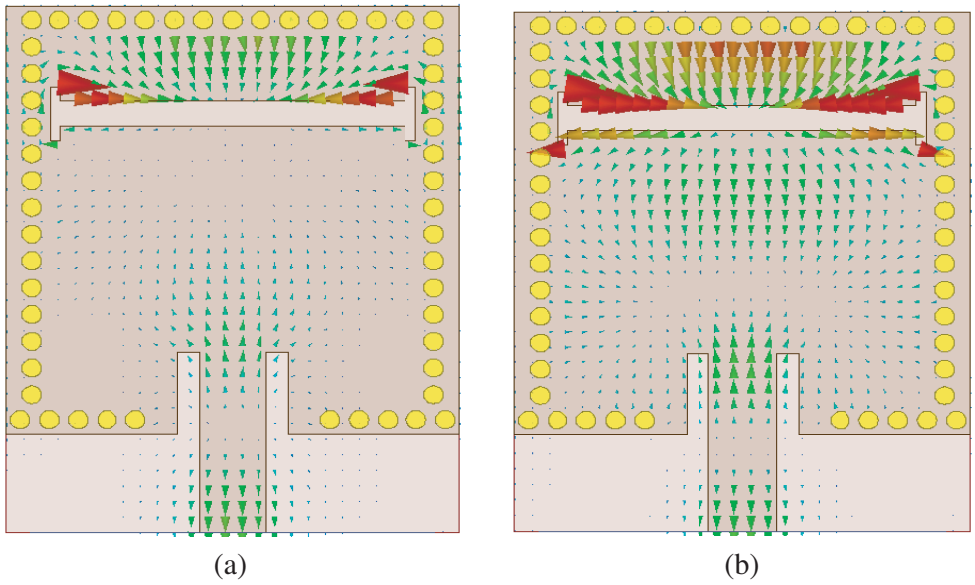

Figure 6. Simulated current density of the proposed structure. (a) 9.6 GHz. (b) 10.6 GHz.

flows to the two sides of the slot. In addition, the E-field strengths at the two sides of an I-shaped slot are different in magnitude and phase, which can make the slot emanate electromagnetic waves into air. The comparison of simulated S_{11} of step II and step III is shown in Figure 7.

4. PARAMETRIC STUDY

To explicate the outcome of different key parameters in the antenna performance, a parametric test is conducted in Figures 8–9 using the HFSS tool. Key parameters are symbolically indicated in Figure 1. During the analysis, the studied parameter is varied while all other parameters are fixed. Primarily, the dimensions of the slot loaded into the SIW cavity are optimized by performing this parametric analysis. When the slot width is altered as depicted in Figure 8(a), the impedance matching is significantly affected, but its center frequency is almost unchanged. With the variations of slot length from 17 mm to 19 mm, the lower resonance (f_1) is decreased. However, the upper resonance f_2 remains unchanged

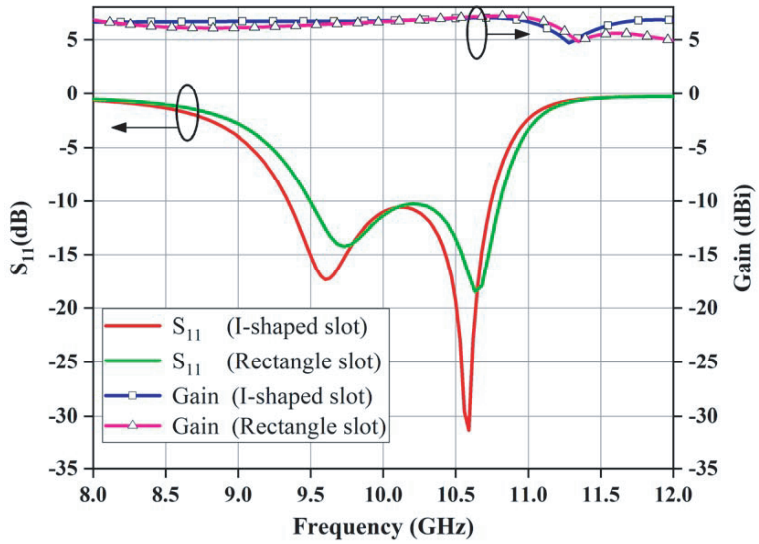

Figure 7. Comparison of simulated S_{11} and gain of I-shaped slot and rectangle slot.

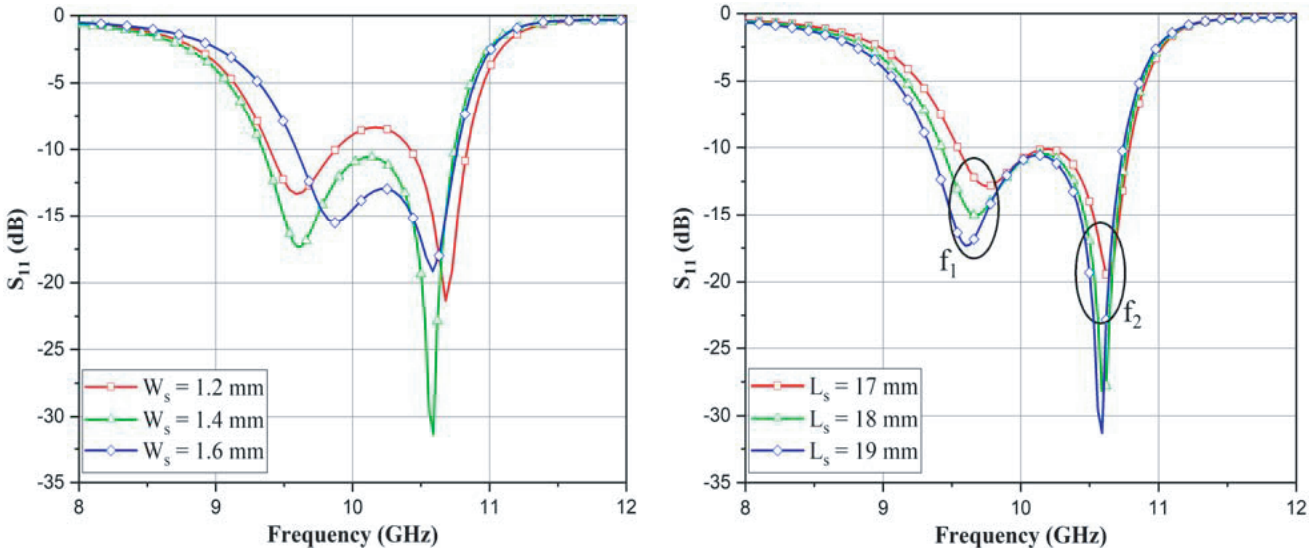

Figure 8. Variation of the S_{11} by changing slot size. (a) W_s. (b) L_s.

in the response. As a result, both S_{11} and impedance bandwidth are improved in the desired frequency band. It is also clear from Figure 8(b) that there is no loading of the slot on even TE_{210} mode while odd TE_{210} mode is greatly affected by the loading of the slot.

As shown in Figure 9(a), when the slot position d_{su} is changed from 4.35 mm to 4.75 mm, excited modes come in close range, as a result, the S_{11} and bandwidth of the antenna are improved. When the substrate thickness increases, the impedance bandwidth of the proposed design is enhanced up to 14% as shown in Figure 9(b). It is a well-known fact that the antenna bandwidth is directly proportional to the substrate thickness. Therefore, $h = 1.57$ mm is selected as substrate thickness. At long last, it is concluded that this parametric investigation sets forth the design to have greater adaptability for the antenna designer.

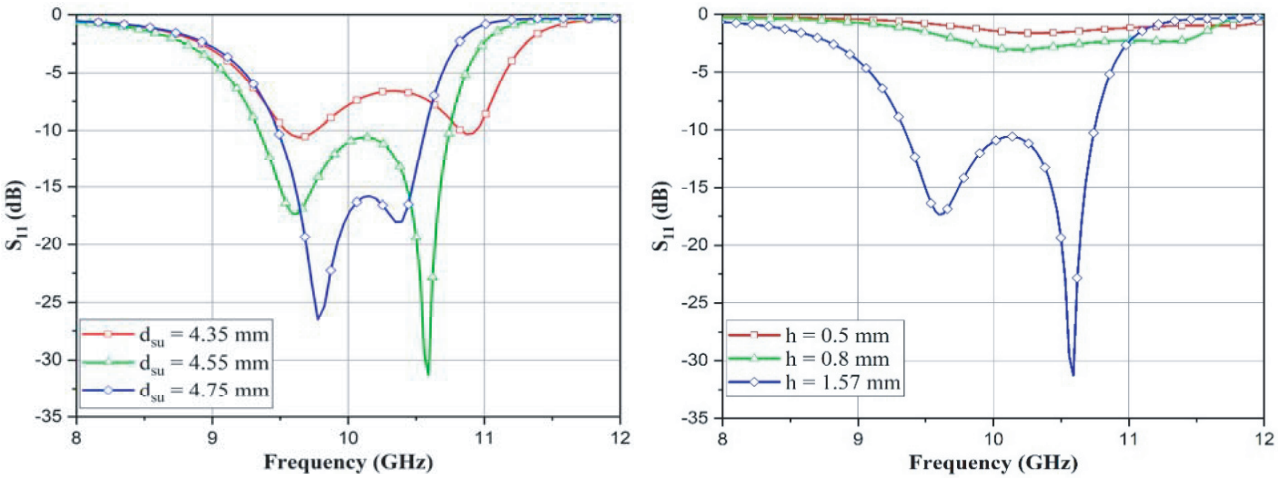

(a) (b)

Figure 9. Variation of the S_{11} by changing. (a) d_{su}. (b) h.

5. RESULTS AND DISCUSSION

To verify the proposed antenna, a prototype is fabricated and tested. Figures 10(a) and (b) show the sample's photographs with front and back views, respectively. The reflection coefficient (S_{11}) is measured by Anritsu MS2037C network analyzer. Measured and simulated results of the S_{11} and gain confirm the wideband response as plotted in Figure 11. The two resonances of the simulated structure are obtained at 9.6 GHz and 10.6 GHz, while those for the measured one are at 9.65 GHz and 10.57 GHz, respectively. Simulated bandwidth (for below -10 dB) is 1.4 GHz (13.94%) while the measured one is 1.45 GHz (14.4%), lying between 9.33 GHz and 10.78 GHz. The simulated and measured S_{11} differ slightly and can be indorsed by the discrepancies taking place in fabrication errors/tolerances and soldering losses. The measured peak gain, at 9.6 GHz is 6.7 dBi and at 10.6 GHz is 7.2 dBi, which are near the simulated findings.

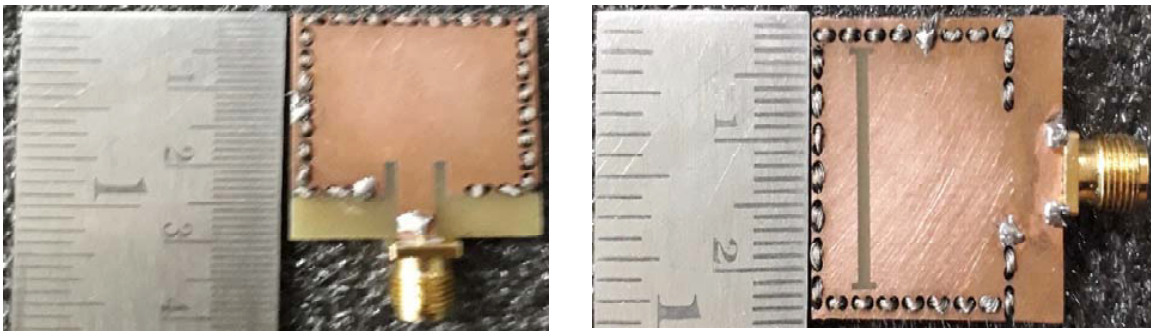

(a) (b)

Figure 10. Fabricated sample. (a) Front view. (b) Back view.

Radiation patterns of the proposed design are depicted in Figure 12, at two different frequencies in two orthogonal planes (XZ-plane ($\varphi = 0°$), YZ-plane ($\varphi = 90°$)). Simulated maximum cross-polarized radiation at 9.6 GHz and 10.6 GHz, is -41 dB and -37 dB, respectively, in XZ-plane, and -24 dB and -20 dB in YZ-plane in the direction of maximum radiation. Measured cross-polarization levels of less than -20 dB are observed at both the frequencies in both the XZ- and YZ-planes. The antenna renders unidirectional radiation, due to the cavity-backed structure and observed maximum radiation toward a positive radiating direction ($90° \leq \theta \leq 270°$). To highlight the contribution of the proposed work, a comparison of our antenna and other similar antennas is listed in Table 1.

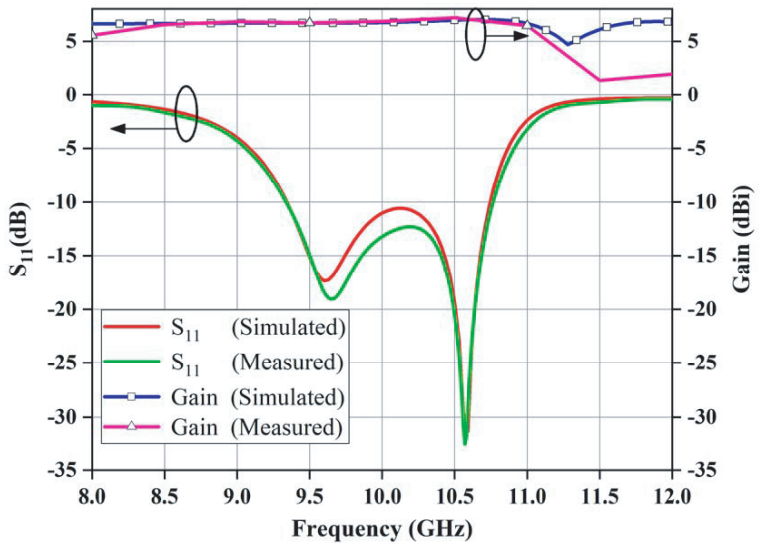

Figure 11. Measured and simulated S_{11} and gain at boresight direction of the proposed antenna.

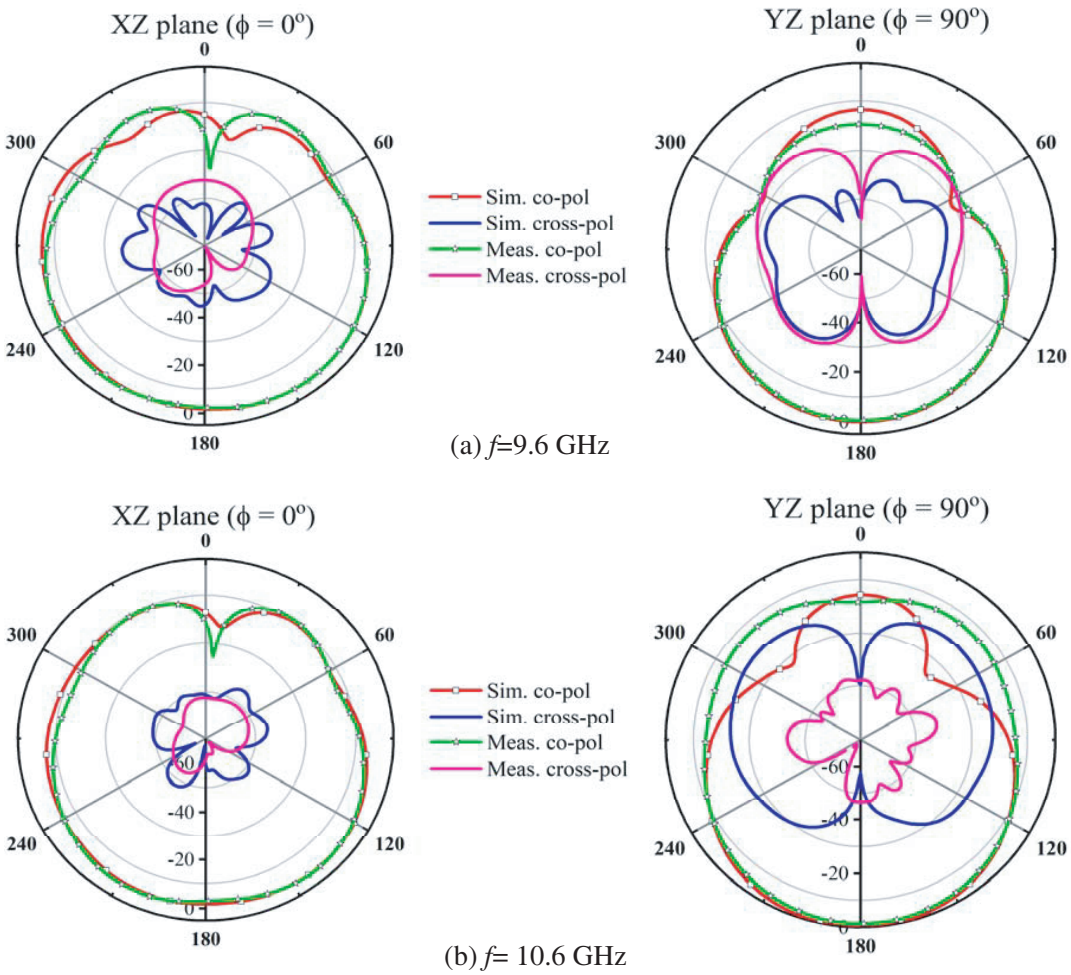

Figure 12. Measured and simulated normalized radiation patterns at (a) 9.6 GHz, and (b) 10.6 GHz.

Table 1. Comparison of our work and other reported antennas.

References	Year	Freq. band	FBW (%)	Gain (dBi)	Cross-pol (dB)	Structure	h (mm)	ε_r
[9]	2008	X	1.7	5.4	−19	Simple	0.5	2.2
[10]	2012	X	6.3	6	−29	Simple	0.5	2.2
[12]	2014	X	9.4	3.7	−18	Complex	0.787	2.2
[14]	2014	X	8	7.9	−16	Complex	0.787	2.2
[20]	2021	X	12.1	6.6	−20	Complex	1.6	2.2
[21]	2021	X	14	7.9	−21	Complex	0.787	2.2
[24]	2014	X	11.2	8	NM	Complex	1.5	2.55
[25]	2013	X	10.9	7.7	−20	Complex	1.016	2.2
This work	2022	X	14.4	7.2	−37	Simple	1.57	2.2

Freq. band: Frequency band; FBW: Fractional Bandwidth; NM: Not Mentioned

6. CONCLUSION

In this article, a bandwidth-enhanced SIW based slot antenna is designed and analyzed. A microstrip line feeding is incorporated into the antenna to excite the SIW cavity. A simple rectangular slot is lodged at the bottom plane for radiating electromagnetic waves. Subsequently, the TE_{210} mode is apportioned into odd and even TE_{210}, which results in more impedance bandwidth. Later, it is modified to an I-shaped structure to attain further bandwidth improvement. Simulated and measured results show impedance bandwidths of 13.94% and 14.4%, respectively. Good agreement has been achieved between the simulated and measured results. The antenna also possesses the benefits, e.g., low profile, light weight, easy fabrication, and high gain.

REFERENCES

1. Yoshimura, Y., "A microstrip slot antenna," *IEEE Trans. on Microw. Theory and Tech.*, Vol. 20, No. 11, 760–762, 1972.
2. Shinde, P. N. and J. P. Shinde, "Design of compact pentagonal slot antenna with bandwidth enhancement for multiband wireless applications," *AEU — Int. J. Electron. Commun.*, Vol. 69, No. 10, 1489–1494, 2015.
3. Kunwar, A., A. K. Gautam, and K. Rambabu, "Design of a compact U-shaped slot triple band antenna for WLAN/WiMAX applications," *AEU — Int. J. Electron. Commun.*, Vol. 71, 82–88, 2017.
4. Lin, J. F. and Q. X. Chu, "Increasing bandwidth of slot antennas with combined characteristic modes," *IEEE Trans. Antennas Propag.*, Vol. 66, No. 6, 3148–3153, 2018.
5. Bozzi, M., A. Geordiadis, and K. Wu, "Review of substrate-integrated waveguide circuits and antennas," *IET Microwaves Antennas Propag.*, Vol. 5, No. 8, 909–920, 2011.
6. Kumar, A., G. Saini, and S. Singh, "A review on future planar transmission line," *Cogent Eng.*, Vol. 3, No. 1, 1–12, 2016.
7. Lokeshwar, B., D. Venkatasekhar, and A. Sudhakar, "Wideband low-profile SIW cavity-backed antenna bilateral slots antenna for X-band application," *Progress In Electromagnetics Research M*, Vol. 97, 157–166, 2020.
8. Bollavathi, L., V. Dorai, and S. Alapati, "Wideband planar substrate integrated waveguide cavity-backed amended dumbbell-shaped slot antenna," *AEU — Int. J. Electron. Commun.*, Vol. 127, 153489, 2020.
9. Luo, G. Q., Z. F. Hu, L. X. Dong, and L. L. Sun, "Planar slot antenna backed by substrate integrated waveguide cavity," *IEEE Antennas Wireless Propagat. Lett.*, Vol. 7, 236–239, 2008.

10. Luo, G. Q., Z. F. Hu, W. J. Li, X. H. Zhang, L. L. Sun, and J. F. Zheng, "Bandwidth enhanced low-profile cavity-backed slot antenna by using hybrid SIW cavity modes," *IEEE Trans. Antennas Propag.*, Vol. 60, 1698–1704, 2012.
11. Mukherjee, S., A. Biswas, and K. V. Srivastava, "Bandwidth enhancement of substrate integrated waveguide cavity backed slot antenna by offset feeding technique," *IEEE Appl. Electromagn. Conf.*, 1–2, 2013.
12. Mukherjee, S., A. Biswas, and K. V. Srivastava, "Broadband substrate integrated waveguide cavity-backed bow-tie slot antenna," *IEEE Antennas Wireless Propagat. Lett.*, Vol. 13, 1152–1155, 2014.
13. Baghernia, E. and M. H. Neshati, "Development of a broadband substrate integrated waveguide cavity backed slot antenna using perturbation technique," *Appl. Comput. Electromagn. Soc. J.*, Vol. 29, 847–855, 2014.
14. Varnoosfadetrani, M. V., J. Lu, and B. Zhu, "Matching slot role in bandwidth enhancement of SIW cavity-backed slot antenna," *Asia-Pacific Conf. on Antennas and Propag.*, 244–247, 2014.
15. Dashti, H. and M. H. Neshati, "Development of low profile patch and semi-circular SIW cavity hybrid antennas," *IEEE Trans. Antennas Propag.*, Vol. 62, No. 9, 4481–4488, 2014.
16. Kumar, A. and S. Raghavan, "Wideband slotted substrate integrated waveguide cavity backed antenna for Ku-band application," *Microwave Opt. Technol. Lett.*, Vol. 59, No. 7, 1613–1619, 2017.
17. Heydarzadeh, F. and M. H. Neshati, "Design and development a wideband SIW based cavity-backed slot antenna using two symmetrical circular corner perturbations," *Int. J. RF Microw. Comput. Aided Eng.*, Vol. 28, No. 9, e21552, 2018.
18. Niu, B. J. and J. H. Tan, "Bandwidth enhancement of low-profile SIW cavity antenna with bilateral slots," *Progress In Electromagnetics Research Letters*, Vol. 82, 25–32, 2019.
19. Feng, C., J. Yang, L. Yan, Y. Zhang, Y. Geng, and W. Zhang, "Broadband substrate-integrated waveguide slot antenna," *Electromagnetics*, Vol. 32, No. 5, 294–304, 2012.
20. Lokeshwar, B., D. Venkatasekhar, and A. Sudhakar, "Development of a low-profile broadband cavity backed bow-tie shaped slot antenna in SIW technology," *Progress In Electromagnetics Research Letters*, Vol. 100, 9–17, 2021.
21. Sarani, A. V., M. H. Neshati, and M. Fazaelifar, "Development of a wideband hexagonal SIW cavity-backed slot antenna array," *AEU — Int. J. Electron. Commun.*, Vol. 139, 153915, 2021.
22. Chaturvedi, D., "SIW cavity-backed 24° inclined-slots antenna for ISM band application," *Int. J. RF Microw. Comput. Aided Eng.*, Vol. 30, e22160, 2020.
23. Ali, H. A., E. Massoni, L. Silvestri, M. Bozzi, L. Perregrini, and A. Gharsallah, "Increasing the bandwidth of cavity-backed SIW antennas by using stacked cavities," *Int. J. Microw. Wirel. Tech.*, Vol. 10, No. 8, 942–947, 2018.
24. Liu, L., H. Wang, Z. Zhang, Y. Li, and Z. Feng, "Wideband substrate integrated waveguide cavity-backed spiral shaped patch antenna," *Microw. Opt. Technol. Lett.*, Vol. 57, No. 2, 332–337, 2015.
25. Yang, W. and J. Zhou, "Wideband low profile substrate integrated waveguide cavity backed E-shaped patch antenna," *IEEE Antennas Wireless Propagat. Lett.*, Vol. 12, 143–146, 2013.
26. Yun, S., D. Y. Kim, and S. Nam, "Bandwidth enhancement of cavity backed slot antenna using a via-hole above the slot," *IEEE Antenna Wireless Propagat. Lett.*, Vol. 11, 1092–1095, 2012.
27. Yun, S., D. Y. Kim, and S. Nam, "Bandwidth and efficiency enhancement of cavity-backed slot antenna using a substrate removal," *IEEE Anten. Wirel. Propagat. Lett.*, Vol. 11, 1458–1461, 2012.
28. Shi, Y., J. Liu, and Y. Long, "Wideband triple- and quad-resonance substrate integrated waveguide cavity-backed slot antennas with shorting vias," *IEEE Trans. Antennas Propag.*, Vol. 65, No. 11, 5768–5775, 2017.
29. Wu, Q., J. Yin, C. Yu, H. Wang, and W. Hong, "Broadband planar SIW cavity-backed slot antennas aided by unbalanced shorting vias," *IEEE Antennas Wireless Propagat. Lett.*, Vol. 18, No. 2, 363–367, 2019.
30. Lokeshwar, B., D. Venkatasekhar, and A. Sudhakar, "Dual-band low profile SIW cavity-backed antenna by using bilateral slots," *Progress In Electromagnetics Research C*, Vol. 100, 263–273, 2020.